

DOUBLY-PERIODIC PROGRESSIVE PERMANENT WAVES IN DEEP WATER

by

P.J. Bryant

No. 35

July 1984

## DOUBLY-PERIODIC PROGRESSIVE PERMANENT WAVES IN DEEP WATER

By P.J. BRYANT

Mathematics Department, University of Canterbury, Christchurch, New Zealand

The Stokes wave is generalized to progressive waves in deep water which are periodic in two orthogonal directions, and are steady relative to a frame of reference moving in one of these directions. These doubly-periodic waves are nonlinear at their lowest approximation, and are calculated from the nonlinear equations for irrotational motion in deep water. It is shown how doubly-periodic waves of small but finite wave slope may be calculated also from the nonlinear Schrödinger equation. The three dimensional paths of particles on the free surface of a doubly-periodic wave are found, and the interesting property is demonstrated that the mean particle paths differ from the direction of advance of the wave crests. The upper boundary of occurrence of doubly-periodic waves at the smaller wavelength ratios is identified with the stability boundary for Stokes waves. Doubly-periodic waves are believed to be a closer approximation than Stokes waves to local wave structures on the ocean.

1. INTRODUCTION

The gravity wave motion on the ocean surface consists of waves, generated at a number of sources, which interact and decay as they propagate across the surface. The local ocean wave spectrum has peaks, therefore, which may be identified with wave trains propagating in different directions. The Stokes wave is a periodic wave train of symmetric permanent shape propagating in one direction for which the water surface displacement is described by

$$\eta = \sum_{k=0}^{\infty} a_k \cos k(x - ct) . \quad (1.1)$$

This Fourier cosine series, with constant Fourier amplitudes  $a_k$ , has permanent shape in a frame of reference moving with the wave velocity  $c$  in the  $x$ -direction. The present investigation is concerned with generalizing the Stokes wave to progressive waves of permanent shape which are periodic in two horizontal directions.

A doubly-periodic progressive permanent wave is described by

$$\eta = \sum_{j=0}^{\infty} \sum_{k=-\infty}^{\infty} a_{jk} \cos\left\{ \frac{j}{r} [(x - ct) \cos\alpha + y \sin\alpha] + k [(x - ct) \cos\beta + y \sin\beta] \right\}, \quad (1.2)$$

a double Fourier cosine series with constant Fourier amplitudes  $a_{jk}$ , which has permanent shape in a frame of reference moving with velocity  $c$  in the  $x$ -direction. This wave is periodic in the two oblique directions defined by  $x \cos\alpha + y \sin\alpha = \text{constant}$ , and  $x \cos\beta + y \sin\beta = \text{constant}$ . It is composed of two wave trains of wavelength ratio  $r$  propagating at angles  $\alpha$  and  $\beta$  to the  $x$ -direction together with their nonlinear interaction. The permanent shape is equivalent to the two wave trains being locked together in the  $x$ -direction.

The locking of the two wave trains can occur only if the nonlinear dispersion relation for gravity waves is applicable, with dependence on wave amplitude as well as wavelength. This property implies that doubly-periodic waves are nonlinear at their lowest approximation. The investigation of long-crested waves by Roberts & Peregrine (1983), using a perturbation expansion which appears to be linear at its lowest approximation, is in fact nonlinear there because it contains a wave amplitude in the linear solution which is determined by a secularity condition at the third order.

The first calculations of doubly-periodic permanent waves appear to be those by Saffman & Yuen (1980), who considered the bifurcation of a Stokes wave into permanent waves with dependence on two horizontal coordinates. They obtained two forms of wave solution described as

symmetrical and skewed. The symmetrical form is progressive in the x-direction, standing in the y-direction, and is singly-periodic. The skewed form corresponds to equation (1.2) with  $\beta = 0$ , it is progressive in the x-direction, and is doubly-periodic in the y-direction and in a direction  $\frac{1}{2}\pi + \alpha$  with the x-axis (Saffman & Yuen (1980), §4, with  $r, \alpha$  above related to their  $p, q$  by  $(1/r)\cos\alpha = p$ ,  $(1/r)\sin\alpha = q$ ). The undisturbed Stokes wave in their formulation propagates in the x-direction, when it is described by the waveband  $j = 0$  in equation (1.2) with  $\beta = 0$ , and the modulation is represented by the wave components with  $k = 0$ ,  $j > 0$  in this equation. Their use of the Zakharov equation led to the neglect of interactions between higher harmonics of the undisturbed Stokes wave and the modulations, equivalent in equation (1.2) to  $a_{jk} = 0$  for  $j > 0$ ,  $|k| > 1$ .

Meiron, Saffman, & Yuen (1982) and Roberts & Schwartz (1983) made more accurate calculations of the symmetrical progressive-standing waves. Their method is similar to that described below (§2), except that it is based on collocation rather than on Fourier transforms. Ma (1982) used a more general form of the Zakharov equation to calculate bifurcations to Stokes waves. His representation is the particular case of equation (1.2) with  $\beta = 0$  for which  $a_{jk} = 0$ ,  $j > 1$ , which is equivalent to linearization in the modulation. Martin (1982) found symmetrical and skewed wave solutions of the nonlinear Schrödinger equation having the same form as those of Saffman & Yuen (1980).

Roberts (1983) used a perturbation expansion in the wave slope to calculate short-crested symmetrical progressive-standing wave solutions of Laplace's equation with the nonlinear free surface boundary conditions (equations (2.1) below). This approach complements the solutions by collocation referred to above, and was used also by Roberts & Peregrine (1983) to calculate long-crested progressive-standing wave solutions. The latter investigation is discussed in §§4,5 below.

The doubly-periodic waves calculated here are the simple case given by  $\alpha = \frac{1}{2}\pi$ ,  $\beta = 0$  in equation (1.2), namely

$$\eta = \sum_{j=0}^{\infty} \sum_{k=-\infty}^{\infty} a_{jk} \cos\{(j/r)y + k(x-ct)\}, \quad (1.3)$$

which are periodic in the  $x$  and  $y$  directions. An example of such a wave is sketched in perspective in figure 1, showing 4 wavelengths in the  $x$ -direction and 2 wavelengths in the  $y$ -direction, with  $r = 4$ . The wave has permanent shape relative to a frame of reference moving in the  $x$ -direction, and the straight-crested part of the wave progresses at  $10.5^\circ$  to the  $x$ -direction. It is demonstrated in §6 how the particle paths are three dimensional with a mean direction for the straight-crested parts which is inclined at only  $0.8^\circ$  to the  $x$ -direction. The structure at the ends of the crests is shown in greater detail in the upper part of the figure. The minimum wave height (trough to crest) at the ends of the crests is 0.53 of the maximum wave height of the straight-crested part.

Attention is drawn to the similarity in appearance between figure 1 and the wave patterns generated experimentally by Su (1982, figure 4). His wave patterns are part of an evolving wave field, rather than the steady wave patterns calculated here. Nevertheless, the qualitative similarity gives confidence in the physical relevance of doubly-periodic waves.

## 2. CALCULATION OF DOUBLY-PERIODIC WAVES

The set of equations describing gravity waves in inviscid irrotational motion in deep water is

$$\phi_{xx} + \phi_{yy} + \phi_{zz} = 0, \quad z < \varepsilon\eta(x,y,t), \quad (2.1a)$$

$$\phi_x, \phi_y, \phi_z \rightarrow 0, \quad z \rightarrow -\infty, \quad (2.1b)$$

$$\eta_t - \phi_z + \varepsilon\eta_x\phi_x + \varepsilon\eta_y\phi_y = 0, \quad z = \varepsilon\eta(x,y,t), \quad (2.1c)$$

$$\eta + \phi_t + \frac{1}{2}\varepsilon(\phi_x^2 + \phi_y^2 + \phi_z^2) = 0, \quad z = \varepsilon\eta(x,y,t). \quad (2.1d)$$

The dimensional variables are the water surface displacement  $a\eta$ , the velocity potential  $(g\ell)^{\frac{1}{2}}a\phi$ , and  $\ell x, \ell y, \ell z$ ,  $(\ell/g)^{\frac{1}{2}}t$ , where  $a$  is the maximum wave height  $\eta(0,0,0)$ ,  $2\pi\ell$  is the wavelength in the  $x$ -direction, and  $\varepsilon = a/\ell$  is a measure of wave slope. The origin of coordinates lies in the mean free surface with the  $z$ -axis vertically upwards.

The nondimensional description of the simple doubly-periodic permanent wave (equation 1.3) is

$$\eta = \sum_{j=0}^J \sum_{k=k_1(j)}^{k_2(j)} a_{jk} \cos\{(j/r)y + k(x-ct)\}, \quad (2.2a)$$

which is a wave train with wavelengths  $2\pi\ell$  in the  $x$ -direction,  $2\pi r\ell$  in the  $y$ -direction, whose shape is steady relative to a frame of reference moving with velocity  $c(g\ell)^{\frac{1}{2}}$  in the  $x$ -direction. The bounds of summation are determined numerically by trial and error so that the set of amplitudes  $a_{jk}$  includes all those amplitudes greater in magnitude than some small prescribed value (usually  $10^{-4}$ ). Since  $\eta$  is chosen to have a zero mean, the lower bound  $k_1(0)$  may be set equal to 1. Other lower bounds  $k_1(j)$ ,  $j > 0$  may be negative. The associated solution of Laplace's equation (2.1a) is

$$\phi = \sum_{j=0}^J \sum_{k=k_1(j)}^{k_2(j)} b_{jk} \exp\{((j/r)^2 + k^2)^{\frac{1}{2}}z\} \sin\{(j/r)y + k(x-ct)\}. \quad (2.2b)$$

The set of amplitudes  $a_{jk}$ ,  $b_{jk}$  (all  $j,k$ ) and the nondimensional wave velocity  $c$  are unknown functions of the wave slope parameter  $\varepsilon$  and the wavelength ratio  $r$ .

Equations (2.2) describe one particular family of doubly-periodic waves, probably the simplest family. These equations are numerically complete in the sense that they include a complete set of wave components, greater in magnitude than some small prescribed value, which are generated by the nonlinear interactions contained in equations (2.1c,d).

The solution method is the same as that applied to oblique wave groups in deep water (Bryant, 1984), where more details about the method

may be found. Equations (2.2a,b) are substituted into equations (2.1c,d), with  $c_{jk}$  denoting the cosine in equation (2.2a) and  $s_{jk}$  the sine in equation (2.2b), giving

$$\begin{aligned}
 F &= \sum_j \sum_k \{ k c a_{jk} s_{jk} - ((j/r)^2 + k^2)^{\frac{1}{2}} b_{jk} \exp\{\varepsilon((j/r)^2 + k^2)^{\frac{1}{2}} \eta\} s_{jk} \} \\
 &- \varepsilon \sum_j \sum_k k a_{jk} s_{jk} \times \sum_j \sum_k k b_{jk} \exp\{\varepsilon((j/r)^2 + k^2)^{\frac{1}{2}} \eta\} c_{jk} \\
 &- \varepsilon \sum_j \sum_k (j/r) a_{jk} s_{jk} \times \sum_j \sum_k (j/r) b_{jk} \exp\{\varepsilon((j/r)^2 + k^2)^{\frac{1}{2}} \eta\} c_{jk} = 0,
 \end{aligned} \tag{2.3a}$$

$$\begin{aligned}
 G &= \sum_j \sum_k \{ a_{jk} c_{jk} - k c b_{jk} \exp\{\varepsilon((j/r)^2 + k^2)^{\frac{1}{2}} \eta\} c_{jk} \} \\
 &+ \frac{1}{2} \varepsilon \left( \sum_j \sum_k k b_{jk} \exp\{\varepsilon((j/r)^2 + k^2)^{\frac{1}{2}} \eta\} c_{jk} \right)^2 \\
 &\quad + \frac{1}{2} \varepsilon \left( \sum_j \sum_k (j/r) b_{jk} \exp\{\varepsilon((j/r)^2 + k^2)^{\frac{1}{2}} \eta\} c_{jk} \right)^2 \\
 &+ \frac{1}{2} \varepsilon \left( \sum_j \sum_k ((j/r)^2 + k^2)^{\frac{1}{2}} b_{jk} \exp\{\varepsilon((j/r)^2 + k^2)^{\frac{1}{2}} \eta\} s_{jk} \right)^2 = 0,
 \end{aligned} \tag{2.3b}$$

where  $\exp\{\varepsilon((j/r)^2 + k^2)^{\frac{1}{2}} \eta\} = \exp\{\varepsilon((j/r)^2 + k^2)^{\frac{1}{2}} \sum_p \sum_q a_{pq} c_{pq}\}$ . Also

$$H = \sum_j \sum_k a_{jk} - 1 = 0 \tag{2.3c}$$

because the maximum nondimensional surface displacement  $\eta(0,0,0)$  is taken to be 1. Equations (2.3a,b) are calculated at a grid of points in  $x-ct, y/r$  space, and with fast Fourier transforms are reduced numerically to

$$F = \sum_m \sum_n F_{mn} s_{mn} = 0, \tag{2.4a}$$

$$G = \sum_m \sum_n G_{mn} c_{mn} = 0, \tag{2.4b}$$

$$\text{from which } F_{mn} = G_{mn} = 0, \quad \text{all } m,n. \tag{2.5}$$

The Fourier coefficients  $F_{mn}, G_{mn}$  are nonlinear functions of  $a_{jk}, b_{jk}$  (all  $j$  and  $k$ ) and  $c$  for given  $\varepsilon$  and  $r$ . Fourier transforms are calculated for the derivatives of  $F, G$  and  $H$  with respect to  $a_{jk}, b_{jk}$  (all  $j$  and  $k$ ) and  $c$ . Newton's method is used then in the Fourier transform space to calculate  $a_{jk}, b_{jk}$  (all  $j$  and  $k$ ) and  $c$  as solutions of equations

(2.3a,b,c) on the grid of points used for the Fourier transforms. All calculations were performed in double precision on a Prime 750 computer, with subroutines adapted from the Harwell Subroutine Library.

### 3. OCCURRENCE OF DOUBLY-PERIODIC WAVES

Doubly-periodic waves are calculated as functions of  $\varepsilon$  and  $r$  by making step by step changes in either  $\varepsilon$  or  $r$  to find new solutions from old solutions. For any given value of the wavelength ratio  $r$ , doubly-periodic waves of the form described by equations (2.2) exist for values of the wave slope parameter  $\varepsilon$  greater than some positive minimum. As  $\varepsilon$  approaches the minimum value from above, the doubly-periodic waves tend towards a Stokes wave propagating in a direction  $\theta_0 = \tan^{-1}(1/r)$  with the  $x$ -direction. The wavelength  $2\pi\ell_0$  of the Stokes waves is given

$$\ell_0 = \ell \cos\theta_0 = \ell r / (r^2 + 1)^{\frac{1}{2}}, \quad (3.1)$$

and if the trough to crest height of the Stokes wave is denoted by  $2a_0$ , a more appropriate wave slope parameter for the Stokes wave is

$$\varepsilon_0 = a_0 / \ell_0. \quad (3.2)$$

As  $\varepsilon$  tends to the minimum value from above, the Jacobian in Newton's method increases in magnitude, making it possible to calculate the minimum value of  $\varepsilon$  and the Stokes wave solution there with accuracy. In contrast, calculation of the maximum value of  $\varepsilon$  for any given  $r$  is approximate because the Jacobian in Newton's method decreases in magnitude as this limit is approached.

For values of  $\varepsilon$  greater than the minimum, a more appropriate wave slope parameter may be defined from the wave height and wavelength of the straight-crested parts of the doubly-periodic wave. The wave height  $2a_0$  and wavelength  $2\pi\ell_0$  are both determined from the wave solution once it has been calculated for the given values of  $\varepsilon$  and  $r$ . In the example in figure 1, for which  $\varepsilon = 0.5$ ,  $r = 4$ , these parameters are  $a_0 = 0.394\ell$ ,  $\ell_0 = 0.983\ell$ , making  $\varepsilon_0 = 0.40$ . The minimum value of  $\varepsilon$  for  $r = 4$  is 0.276,

when the Stokes wave there has a wave slope parameter  $\varepsilon_0 = 0.250$ . The maximum value of  $\varepsilon$  when  $r = 4$  is 0.584 approximately, for which the straight-crested parts of the wave have a wave slope parameter  $\varepsilon_0 = 0.437$ .

The basic geometric unit of the doubly-periodic wave structure described by equation (2.2) is a rectangle of sides  $2\pi\ell$  in the x-direction and  $2\pi r\ell$  in the y-direction. The angle  $\tan^{-1}(1/r)$  in this rectangle equals the direction of propagation  $\theta_0$  of the Stokes wave at the minimum value of  $\varepsilon$  for the given value of  $r$ . The wave slope parameter  $\varepsilon_0$  normal to the straight-crested parts of the wave is a more descriptive amplitude parameter than the wave slope parameter  $\varepsilon$  in the x-direction. For these reasons, the region of occurrence of the doubly-periodic waves is sketched in figure 2 in terms of  $\theta_0$  and  $\varepsilon_0$ .

The lower curve in figure 2 has been calculated to within the accuracy of the figure for values of  $\theta_0$  up to about  $60^\circ$ . Wave resonances become significant at greater angles (§7), where the doubly-periodic wave solutions do not appear to be physically relevant. The upper curve in figure 2 is everywhere approximate for the reasons stated above. It could not be extended to values of  $\theta_0$  below about  $5^\circ$  because the number of wave components required to find solutions there exceeded the computing capacity available. The region of occurrence is discussed in three parts, small wave slopes (§5), large wave slopes with  $\theta_0$  small (§6), and large wave slopes with  $\theta_0$  large (§7).

#### 4. NONLINEAR SCHRÖDINGER EQUATION

The nonlinear Schrödinger equation for wave motion on the surface of deep water, using the nondimensional notation defined in §2, is

$$i(A_t + \frac{1}{2}A_x) - \frac{1}{8}A_{xx} + \frac{1}{4}A_{yy} - \frac{1}{2}\varepsilon^2|A|^2A = 0 \quad (4.1a)$$

where

$$\eta = \Re\{A(x,y,t)\exp i(x-t)\}. \quad (4.1b)$$

The equation is valid for waves of small but finite wave slope  $\epsilon$ , for which the amplitude function  $A(x,y,t)$  is a slowly varying function of  $x,y$  and  $t$ . The latter condition is equivalent to the Fourier decomposition of  $\eta$  having a single narrow peak in two dimensional wavenumber space near the wave component of wavenumber 1 in the  $x$ -direction. These conditions are satisfied for doubly-periodic waves near the origin in figure 2, implying that these waves should be modelled by equations (4.1). The analysis below is similar to that derived by Roberts & Peregrine (1983, Appendix).

The amplitude function for the simple doubly-periodic waves described by equation (2.2) is a non-zero function dependent on  $y$  and  $t$  alone,  $A(y,t)$ . Equation (4.1a), with the substitution

$$A(y,t) = F(y) \exp\{i\Phi(y) - i\alpha t\} \quad (4.2)$$

( $F, \Phi, \alpha$  real), followed by cancellation of the exponential functions, has real and imaginary parts

$$F_{YY} - F\Phi_Y^2 + 4\alpha F - 2F^3 = 0, \quad (4.3a)$$

$$F\Phi_{YY} + 2F_Y\Phi_Y = 0. \quad (4.3b)$$

Equation (4.3b) integrates to

$$F^2\Phi_Y = B \quad (4.4)$$

where  $B$  is an arbitrary constant. After substitution for  $\Phi_Y$ , equation (4.3a) becomes

$$F_{YY} - \frac{B^2}{F^3} + 4\alpha F - 2F^3 = 0 \quad (4.5a)$$

which integrates to

$$F_Y^2 = F^4 - 4\alpha F^2 - \frac{B^2}{F^2} + C, \quad (4.5b)$$

where  $C$  is an arbitrary constant.

Equation (4.5b) with  $B = 0$  has no solutions describing a periodic oscillation of  $F(y)$  between positive extrema  $F_1, F_2$ . If  $F_Y$  has zeroes at  $F = F_1, F_2$ , equation (4.5b) with  $B = 0$  has the form

$$F_y^2 = (F_1^2 - F^2)(F_2^2 - F^2), \quad (4.6)$$

which has no real solutions with  $F_1 < F < F_2$ . If  $B$  is nonzero, equation (4.5b) with a suitable choice of  $\alpha, B$ , and  $C$  can have the form

$$F_y^2 = (F^2 - F_0^2)(F_1^2 - F^2)(F_2^2 - F^2)/F^2, \quad (4.7)$$

where  $0 < F_0 < F_1 < F_2$ . Equation (4.7) does have periodic solutions for which  $F_0 \leq F \leq F_1$ . Hence the nonlinear Schrödinger equation (4.1a) can have solutions of the form of equation (4.2) with a positive periodic amplitude  $F(y)$  provided that the phase  $\Phi(y)$  is a monotonically increasing or monotonically decreasing function of  $y$ . The water surface displacement, equation (4.1b), is then

$$\eta = F(y) \cos\{x + \Phi(y) - (1 + \alpha)t\}, \quad (4.8)$$

which is a wave train periodic in the  $x$ -direction, slowly varying in the  $y$ -direction, that is steady relative to a frame of reference moving with a nondimensional velocity  $c = 1 + \alpha$  in the  $x$ -direction. If the wave train is periodic in the  $y$ -direction also, with a nondimensional wavelength  $2\pi r$ , then the solution  $F(y)$  of equations (4.5) has wavelength  $2\pi r$ , and from equation (4.4)

$$B \int_0^{2\pi r} F^{-2} dy = 2\pi \quad (4.9)$$

for the simplest doubly-periodic wave.

Equation (4.5a) may be solved, subject to the constraint (4.9), by a numerical method which is a simplified version of that described in §2 (see also Bryant (1984) §3). Since  $F(y)$  is symmetric in  $y$  with a wavelength  $2\pi r$ , it may be written as the Fourier cosine series

$$F(y) = \frac{1}{2} a_0 + \sum_{k=1}^N a_k \cos(ky/r), \quad (4.10)$$

where  $N$  is determined by trial and error so that the set of amplitudes  $a_k$  includes all those greater in magnitude than some small prescribed value ( $10^{-5}$  here). The Fourier series is substituted into equation (4.5a), which is expanded numerically into a Fourier cosine series at given values

of  $\varepsilon$ ,  $r$ , and  $B$ , and is solved by Newton's method for the  $N + 1$  Fourier amplitudes  $a_0, a_1, \dots, a_N$  and the parameter  $\alpha$ . The constant  $B$  is then changed step by step until the constraint (4.9) is satisfied.

The doubly-periodic wave solutions of the nonlinear Schrödinger equation (4.1) were found to be in good agreement with the corresponding doubly-periodic waves calculated from equations (2.1) at values of  $\varepsilon$  near the origin in figure 2. Some properties of the doubly-periodic wave for which  $\varepsilon = 0.12$ ,  $r = 10$  ( $c = 1.008$ ,  $\varepsilon_0 = 0.096$ ,  $\theta_0 = 5.71^\circ$ ) are sketched in figure 3. The solid curves are derived from equations (2.1) and the dashed curves from the nonlinear Schrödinger equation (4.1). The left hand section shows two transverse wavelengths of the upper and lower wave envelopes, which for the nonlinear Schrödinger equation are  $\pm F(y)$ . The right hand curve is two transverse wavelengths of the wave crest, given for the nonlinear Schrödinger equation by

$$x + \Phi(y) - (1 + \alpha)t = 0 \quad , \quad 1 + \alpha = c \quad (4.11)$$

in equation (4.8). The two solutions coincide within the precision of the figure except for the slight separation of the lower envelopes.

Roberts & Peregrine (1983) calculated long-crested water waves which progress in the  $x$ -direction, are standing waves in the transverse direction, and are doubly-periodic in these two directions. They used a perturbation expansion in wave slope valid for the parameter range  $\varepsilon \sim \theta_0 \ll 1$  (in the present notation). Since their leading order solution has no phase change with respect to the transverse variable, their equations (2.10, 2.11) for the wave amplitude are the same (apart from a scaling factor) as equations (4.5a, b) above with  $B = 0$ . These equations were shown to have sn solutions with envelope zeroes. Their fourth order solutions for doubly-periodic long-crested waves have envelope zeroes also. However, their analysis of the nonlinear Schrödinger equation does admit doubly-periodic progressive wave solutions without envelope zeroes, suggesting

that the perturbation expansion method could be used to calculate doubly-periodic progressive wave solutions without envelope zeroes, for which the leading order solution does have a phase change with respect to the transverse variable.

##### 5. DOUBLY-PERIODIC WAVES OF SMALL WAVE SLOPE

Two properties of doubly-periodic waves of small wave slope are investigated here. Reasons are sought for the right boundary of the region of occurrence of these waves in figure 2 being a straight line through the origin. The form of the doubly-periodic waves as the left boundary is approached, when the wavelength ratio  $r$  becomes large, is examined also.

The right boundary of the region of occurrence in figure 2 is a straight line through the origin of slope 0.877 when  $\theta_0$  is expressed in radians. This boundary is the minimum value of the wave slope parameter  $\varepsilon_0$ , for any given wavelength ratio  $r (= \cot\theta_0)$ , at which two waves at angle  $\theta_0$  may be locked together to form a doubly-periodic wave of permanent shape. The doubly-periodic wave is a Stokes wave at this minimum value, whose dimensional wave velocity, as calculated by Stokes, is

$$c_0 = (g\ell_0)^{\frac{1}{2}} \left( 1 + \frac{1}{2}\varepsilon_0^2 + O(\varepsilon_0^4) \right), \quad (5.1)$$

in the present notation. The nondimensional velocity in the x-direction of a Stokes wave propagating at angle  $\theta_0$  to the x-direction, using equation (3.1), is therefore

$$\begin{aligned} c &= c_0 (g\ell)^{-\frac{1}{2}} (\cos\theta_0)^{-1} \\ &= (\cos\theta_0)^{-\frac{1}{2}} \left( 1 + \frac{1}{2}\varepsilon_0^2 + O(\varepsilon_0^4) \right). \end{aligned} \quad (5.2)$$

This relation is fitted accurately on the whole lower boundary in figure 2.

For values of  $\varepsilon_0$  slightly greater than the minimum value, the doubly-periodic wave in the region of small wave slope consists of the Stokes

wave at angle  $\theta_0$  locked together with a wave component of much smaller magnitude in the x-direction. The drift velocity associated with the Stokes wave, expressed in dimensional form, is

$$v = \kappa c_0 \varepsilon_0^2 \quad (5.3)$$

in the direction of propagation of the Stokes wave, where  $\kappa$  is a dimensionless constant. The non-dimensional velocity in the x-direction of the wave component propagating in this direction on top of the Stokes wave at angle  $\theta_0$  is therefore

$$\begin{aligned} c &= (v \cos \theta_0 + (g\ell)^{\frac{1}{2}}) (g\ell)^{-\frac{1}{2}} \\ &= 1 + \kappa (\cos \theta_0)^{3/2} \varepsilon_0^2 + O(\varepsilon_0^3) . \end{aligned} \quad (5.4)$$

Equations (5.2) and (5.4) are the same for  $\theta_0 \sim \varepsilon_0 \ll 1$ , expressing the locking together of the two waves into the doubly-periodic wave near the right boundary, provided that

$$\varepsilon_0 = (4\kappa - 2)^{-\frac{1}{2}} \theta_0 + O(\theta_0^2) . \quad (5.5)$$

This equation shows that the right boundary is a straight line through the origin for doubly-periodic waves of small wave slope. The dimensionless constant  $\kappa$  has the value 0.825 for the straight line to take the measured slope 0.877.

Analytical reasons have been sought unsuccessfully for the dimensionless constant  $\kappa$  in equation (5.3) being 0.825. The Stokes drift velocity for fluid particles at mean level  $\ell z_0$  is (Lighthill 1978 p280)

$$v = c_0 \varepsilon_0^2 \exp(2z_0) . \quad (5.6)$$

The wave component propagating in the x-direction experiences a weighted average of the particle velocities associated with the Stokes wave at levels near  $z_0 = 0$ , whose net effect is to cause the dimensionless constant  $\kappa$  to have the value found.

An example is presented of a doubly-periodic wave near the left boundary of the region of small wave slope in figure 2. It tests the accuracy there of doubly-periodic wave solutions of the nonlinear Schrödinger

equation, and may be compared with the long-crested wave of infinite transverse wavelength calculated by Roberts & Peregrine (1983). The parameters for the example are  $\varepsilon = 0.1$ ,  $r = 100$  ( $c = 1.0046$ ,  $\varepsilon_0 = 0.095$ ,  $\theta_0 = 0.57^\circ$ ). The solid curves on the left of figure 4 are the central one eighth of a transverse wavelength of the upper and lower envelopes (contracted 32 times). The remaining seven eighths of the transverse wavelength is a wave train of constant height. The minimum separation of the envelopes at the centre is 0.056 of the maximum separation. The solid curve on the right of figure 4 is the central one eighth of a transverse wavelength of a wave crest (contracted 32 times). The remaining seven eighths of the crest is a straight line inclined at  $0.30^\circ$  to the y-direction. The fit between the exact doubly-periodic wave properties and the corresponding properties of solutions of the nonlinear Schrödinger equation is seen in figure 4 to be very good, probably because this example fits well the assumptions made in deriving the nonlinear Schrödinger equation.

The water surface displacement of the central one eighth of a transverse wavelength is sketched in perspective in figure 5. The figure shows good qualitative agreement with the perspective drawing of the long-crested wave of infinite transverse wavelength calculated by Roberts & Peregrine (1983, figure 4). Both examples are steady relative to a frame of reference moving in the x-direction. However, their example is standing in the transverse direction, while the present example, as can be seen in figure 4, has a small progressive component of velocity in the transverse direction. For this reason, a quantitative comparison is not meaningful.

The water surface displacement and velocity potential for the present example (equations 2.2) each contain 263 wave components in 46 wavebands ( $0 \leq j \leq 45$ ), the wavenumber range being  $-5 \leq k \leq 5$ . The maximum Fourier coefficients  $F_{mn}$ ,  $G_{mn}$  not included in the calculation have

magnitude  $2 \times 10^{-4}$ . The maximum magnitude of F and G over the  $128 \times 16$  points used in the final calculation is  $6.8 \times 10^{-3}$ , with a root mean square deviation of F and G from zero of  $8 \times 10^{-4}$ . (A computer listing of the wave components for all examples may be obtained from the author).

## 6. LARGE WAVE SLOPE WITH LARGE WAVELENGTH RATIO

Doubly-periodic waves in the upper left part of the region of occurrence (figure 2) are discussed here. The structure of these waves is the same as that of doubly-periodic waves of small slope, namely, two wave trains locked together. However, because the wave slopes are larger, more wave components are generated by the nonlinear interactions between the two basic wave components. Attention is restricted here to the family of doubly-periodic waves for which the two basic wave components are  $(j = 0, k = 1)$  and  $(j = 1, k = 1)$  in equation (2.2a). Two examples are presented, the first with  $\varepsilon = 0.5$ ,  $r = 4$ , and the second with  $\varepsilon = 0.5$ ,  $r = 10$ .

The doubly-periodic wave with parameters  $\varepsilon = 0.5$ ,  $r = 4$  ( $\varepsilon_0 = 0.400$ ,  $\theta_0 = 14.04^\circ$ ,  $c = 1.0903$ ) is sketched in perspective in figure 1. The structure at the ends of the crests is shown in more detail at the top of the figure, where the minimum wave height (trough to crest) is 0.53 of the maximum wave height of the straight-crested part. The doubly-periodic wave solution of the nonlinear Schrödinger equation with the same parameters as this example was compared with the example, and found to be unsatisfactory, as is expected for this large value of  $\varepsilon$ . The upper envelope  $F(y)$  and the phase  $\Phi(y)$  were both in error at the ends of wave crests, and the lower envelope  $-F(y)$  was well in error throughout the transverse wavelength. The water surface displacement and velocity potential (equations 2.2a,b) each contain 182 wave components in 14 wavebands ( $0 \leq j \leq 13$ ), the wavenumber range being  $-6 \leq k \leq 18$ . The maximum

Fourier components  $F_{mn}$ ,  $G_{mn}$  not included in the calculation have magnitudes  $3 \times 10^{-4}$ . The maximum magnitude of  $F$  and  $G$  over the  $64 \times 32$  points used in the final calculation is  $6.3 \times 10^{-3}$ , with a root mean square deviation of  $F$  and  $G$  from zero of  $1.0 \times 10^{-3}$ .

The projections on the  $(x,z)$  plane of the free surface particle paths at points initially equally spaced across one transverse wavelength are shown on the left of figure 6, and the mean drift velocity in this direction, calculated from particle paths, is drawn on the right of the figure. Each of the fluid particles in the figure lies initially at the free surface on a transverse cross-section extending from the centre of a straight-crested part to the centre of the next straight-crested part of the wave. The mean drift velocity in the transverse direction is uniform in  $y$ . The interesting property is that the angle of mean drift for the straight-crested part of the wave is inclined at only  $0.8^\circ$  to the  $x$ -direction, while the crest itself advances in a direction at  $10.5^\circ$  to the  $x$ -direction. The particle paths are of a spiral shape with a mean direction of advance which is oblique to the direction of advance of the wave crests containing the particles. Particle paths in Stokes waves are orthogonal to wave crests, but this property is not true for the more physically realistic situation in which the waves have a doubly-periodic structure.

The second example is of a doubly-periodic wave with parameters  $\epsilon = 0.5$ ,  $r = 10$  ( $\epsilon_0 = 0.396$ ,  $\theta_0 = 5.71$ ,  $c = 1.0816$ ) and is sketched in perspective in figure 7. The straight-crested part of the wave progresses at  $3.2^\circ$  to the  $x$ -direction, and the minimum wave height (trough to crest) at the ends of the crests is 0.18 of the maximum wave height of the straight-crested part. The free surface particle paths were found to have properties similar to those in the first example. The mean drift at the free surface in the straight-crested part of the wave is inclined at only  $0.1^\circ$  to the  $x$ -direction.

## 7. LARGE WAVE SLOPE WITH SMALL WAVELENGTH RATIO

There is a narrow region in figure 2 for values of  $\theta_0$  greater than about  $20^\circ$ , and for large wave slopes, in which doubly-periodic waves were found to occur. The doubly-periodic waves tend towards Stokes waves as the lower boundary of the region is approached, indicating that within the narrow region the doubly-periodic waves are close approximations to Stokes waves, differing only in that other wave components of much smaller amplitude are locked together with the Stokes wave components. McLean, Ma, Martin, Saffman, & Yuen (1981) and McLean (1982) have calculated the regions of instability of Stokes waves to oblique perturbations, with linearization in the perturbations. The instability is associated with resonance in the sense that certain wave components lie near the linear dispersion relation. The upper boundary of the narrow region calculated here is believed to be the nonlinear generalization of the stability boundary found by the linear stability analysis.

The Stokes wave components here are those for which  $j = k$  in equation (2.2a). A non-dimensional rectangular coordinate system relative to the Stokes wave is defined by

$$X = x + (1/r)y, \quad Y = - (1/r)x + y, \quad (7.1)$$

for which equation (2.2a) becomes

$$\eta = \sum_j \sum_k a_{jk} \cos \left\{ k(X - ct) + \frac{j - k}{1 + r^2} (X + rY) \right\}. \quad (7.2)$$

Linearization (McLean (1982), equation 5) restricts the Stokes wave perturbations to wave components for which

$$j - k = \pm 1 \quad (7.3)$$

in equation (7.2), when the perturbation wavenumbers are

$$p = \frac{1}{1 + r^2}, \quad q = \frac{r}{1 + r^2} \quad (7.4)$$

( $p, q$  in McLean's notation). An example is presented in which a doubly-periodic wave on the upper boundary of the narrow region is interpreted in terms of the linear stability analysis.

The doubly-periodic wave of maximum wave height when  $r = 0.6$  is found to have parameters  $\varepsilon_0 = 0.40$ ,  $\theta_0 = 59.0^\circ$ ,  $h/\lambda = 0.126$  (in McLean's notation), and  $p = 0.74$ ,  $q = 0.44$  from equation (7.4). The instability diagram for a Stokes wave with this value of the wave slope parameter  $h/\lambda$  is sketched by McLean (1982, p322, figure 2e). The instability diagrams for smaller values of  $h/\lambda$  show that Stokes waves are stable to a perturbation with these values of  $p$  and  $q$ . However, at this value of  $h/\lambda$ , the perturbation wavenumbers  $p$  and  $q$  lie just inside the region of class II instability. Although the dominant off-diagonal wave components of this doubly-periodic wave are those for which  $j - k = + 1$ , the components for which  $j - k = + 2$  are of greater magnitude than those for which  $j - k = - 1$ . The restriction (7.3) is not fully applicable therefore, suggesting that this approximate agreement with McLean's calculations is as much as can be expected.

As the wavelength ratio  $r$  is decreased further, equivalent to  $\theta_0$  increasing, certain off-diagonal wave components increase relative to other wave components because of their nearness to linear resonance. Examination of McLean's instability diagrams shows that class I instabilities contribute at the lower values of the wave slope parameter applicable here. These doubly-periodic waves have not been investigated in detail because of the doubtful physical relevance when their wave crests are inclined at large angles to the direction in which the waves have constant shape. It is difficult to visualize a natural generating mechanism whose coherence extends over such large angles.

## 8. GENERALIZATIONS

The doubly-periodic progressive waves studied here are probably the simplest of this kind. They are periodic in two orthogonal directions, and are steady relative to a frame of reference moving in one of these directions. In the course of calculating the waves, other solution branches were found also. One branch consists of waves dominated by the

wave components for which  $(j = 0, k = 1)$  and  $(j = 2, k = 1)$ , with a much smaller  $(j = 1, k = 1)$  component. These doubly-periodic waves have a similar appearance to those described in §§5,6 except that a modulation of twice the transverse wavelength is locked in with them. Another branch consists of waves dominated by wave components of unequal amplitude for which  $(j = 1, k = 1)$  and  $(j = 1, k = -1)$ . These doubly-periodic waves are more symmetric in appearance than those described here.

Some calculations have been made on doubly-periodic waves which are periodic in two non-orthogonal directions. The skewed doubly-periodic waves of Saffman & Yuen (1980), for which

$$\eta = \sum_j \sum_k a_{jk} \cos\left\{\frac{j}{r} [(x - ct) \cos\alpha + y \sin\alpha] + k(x - ct)\right\}, \quad (8.1)$$

were calculated and extended to larger wave slopes than the Zakharov equation permits. The method of calculation was a generalization of that described in §2, using a space-time grid based on the variables  $(x - ct) \cos\alpha + y \sin\alpha$ ,  $x - ct$ . No new properties were found for these non-orthogonal doubly-periodic waves.

The occurrence of different forms for doubly-periodic waves illustrates the known property that the nonlinear dispersion relation for waves in two horizontal directions on deep water admits many possibilities for resonance and for locking together of wave components.

## REFERENCES

- Bryant, P.J. 1984 Oblique wave groups in deep water. *J. Fluid Mech.*  
(to appear)
- Lighthill, J. 1978 *Waves in Fluids*. Cambridge University Press.
- Ma, Yan-Chow 1982 On steady three-dimensional deep water weakly nonlinear gravity waves. *Wave Motion* 4, 113-125.
- Martin, D.U. 1982 Two-dimensional bifurcations of Stokes waves.  
*Wave Motion* 4, 209-219.
- McLean, John W. 1982 Instabilities of finite-amplitude water waves.  
*J. Fluid Mech.* 114, 315-330.
- McLean, J.W., Ma, Y.C., Martin, D.U., Saffman, P.G., & Yuen, H.C. 1981  
Three-dimensional instability of finite-amplitude water waves.  
*Phys. Rev. Lett.* 46, 817-820.
- Meiron, Daniel I., Saffman, Philip G., & Yuen, Henry C. 1982 Calculation  
of steady three-dimensional deep-water waves. *J. Fluid Mech.* 124,  
109-121.
- Roberts, A.J. 1983 Highly nonlinear short-crested water waves.  
*J. Fluid Mech.* 135, 301-321.
- Roberts, A.J. & Peregrine, D.H. 1983 Notes on long-crested water waves.  
*J. Fluid Mech.* 135, 323-335.
- Roberts, A.J. & Schwartz, L.W. 1983 The calculation of nonlinear short-  
crested gravity waves. *Phys. Fluids* 26, 2388-2392.
- Saffman, Philip G., & Yuen, Henry C. 1980 A new type of three-dimensional  
deep-water wave of permanent form. *J. Fluid Mech.* 101, 797-808.
- Su, M.-Y. 1982 Three-dimensional deep-water waves. Part 1. Experimental  
measurement of skew and symmetric wave patterns. *J. Fluid Mech.* 124,  
73-108.

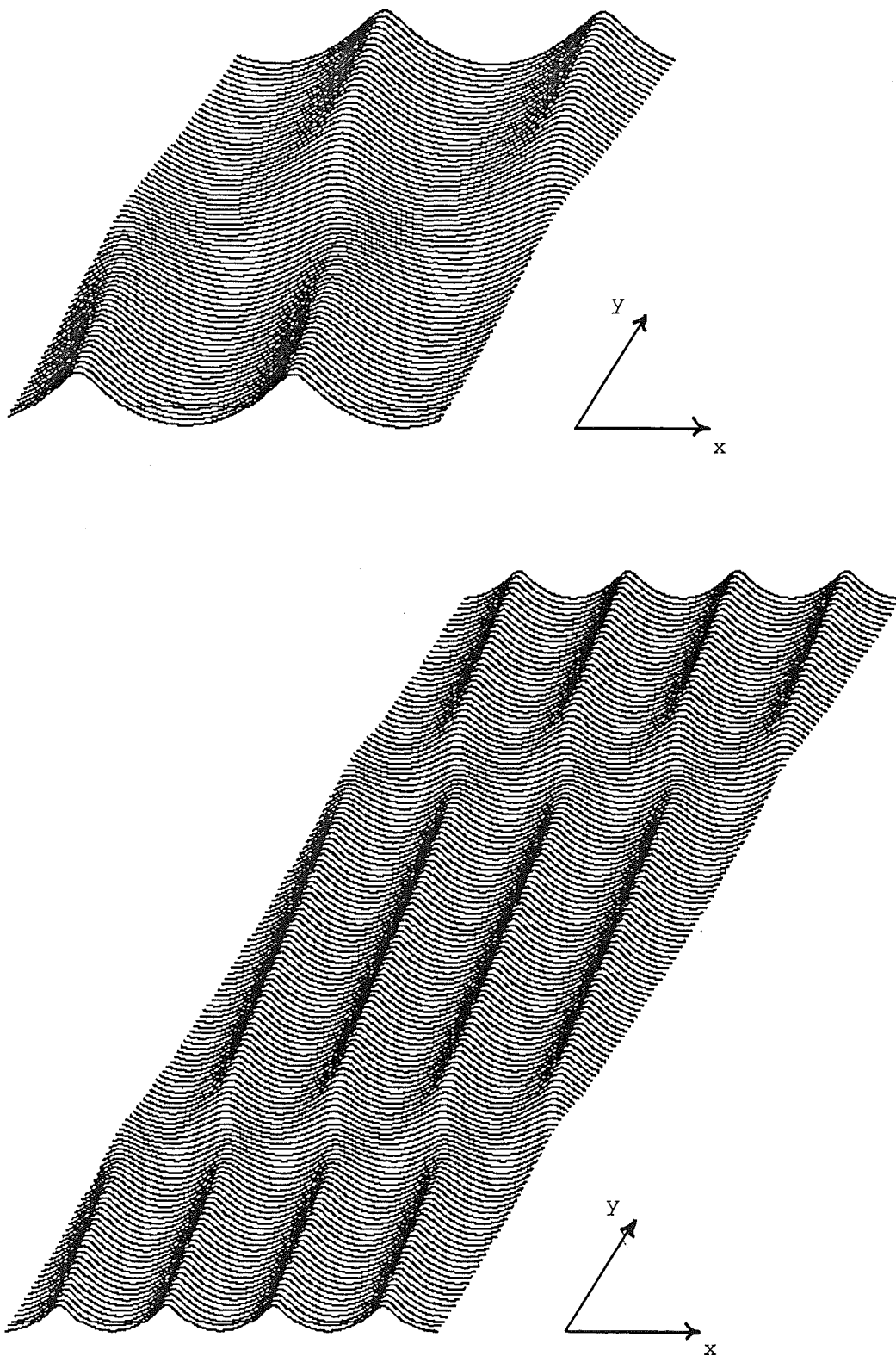


Figure 1 Perspective view of doubly-periodic waves with  $\epsilon = 0.5$ ,  $r = 4$ , showing 4 wavelengths in the x-direction and 2 wavelengths in the y-direction, and a detailed view of the ends of the crests. Vertical magnification 2.

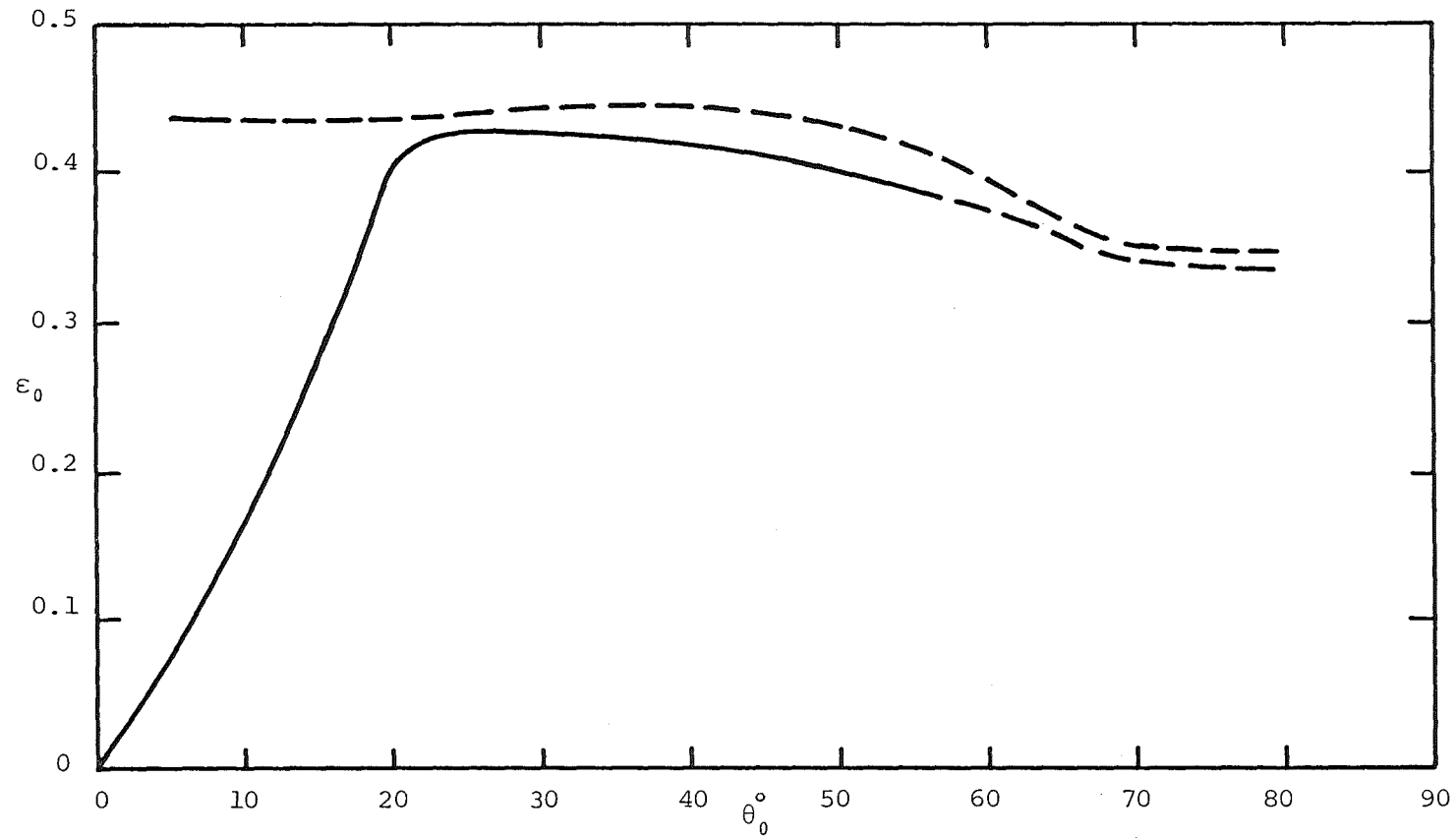


Figure 2 The region of occurrence of doubly-periodic waves in terms of the angle  $\theta_0$  of the basic rectangle and the wave slope parameter  $\epsilon_0$ . The lower boundary is shown as a solid curve where it has been calculated within the precision of the figure.



Figure 3 Comparison of properties of the doubly-periodic wave with  $\varepsilon = 0.12$ ,  $r = 10$  and those of the corresponding solution of the NLS equation. On the left are two transverse wavelengths of the upper and lower envelopes (vertical magnification 20), and on the right are two transverse wavelengths of the wave crest. The dashed curve, distinguishable only on the lower envelope, is the NLS solution.

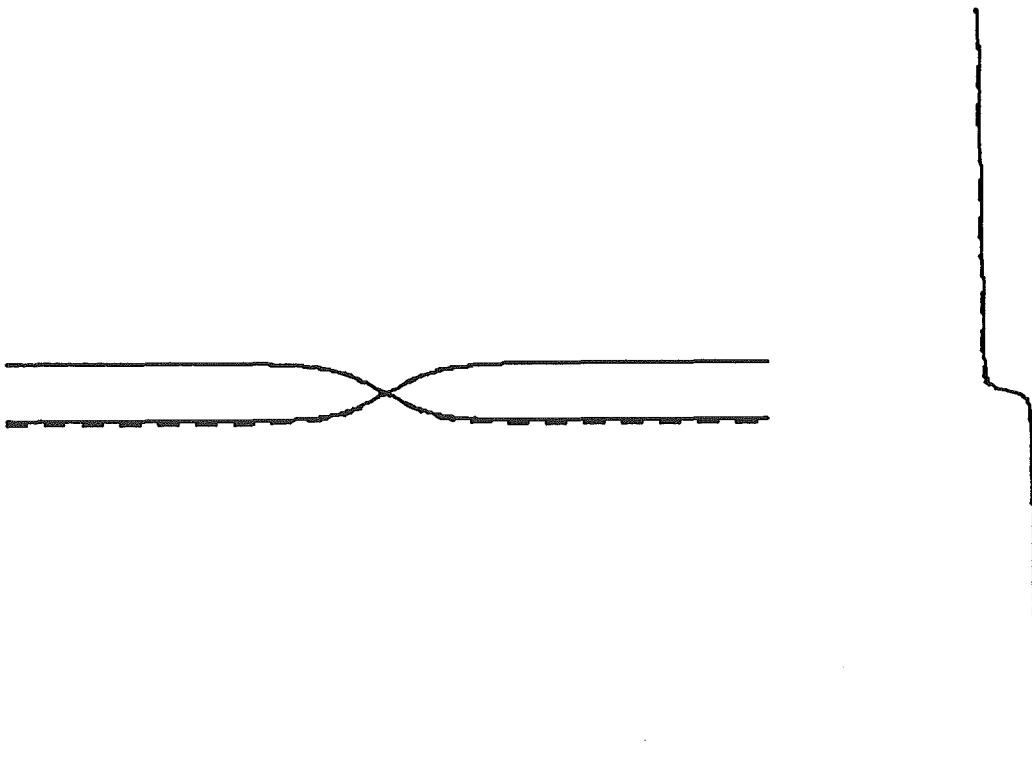


Figure 4 Comparison of properties of the doubly-periodic wave with  $\varepsilon = 0.1$ ,  $r = 100$  and those of the corresponding solution of the NLS equation. On the left is one eighth of a transverse wavelength of the upper and lower envelopes (minimum separation 0.056 of maximum separation), and on the right is one eighth of a transverse wavelength of the wave crest, all contracted 32 times in the transverse direction. The dashed curve, distinguishable only on the lower envelope, is the NLS solution.

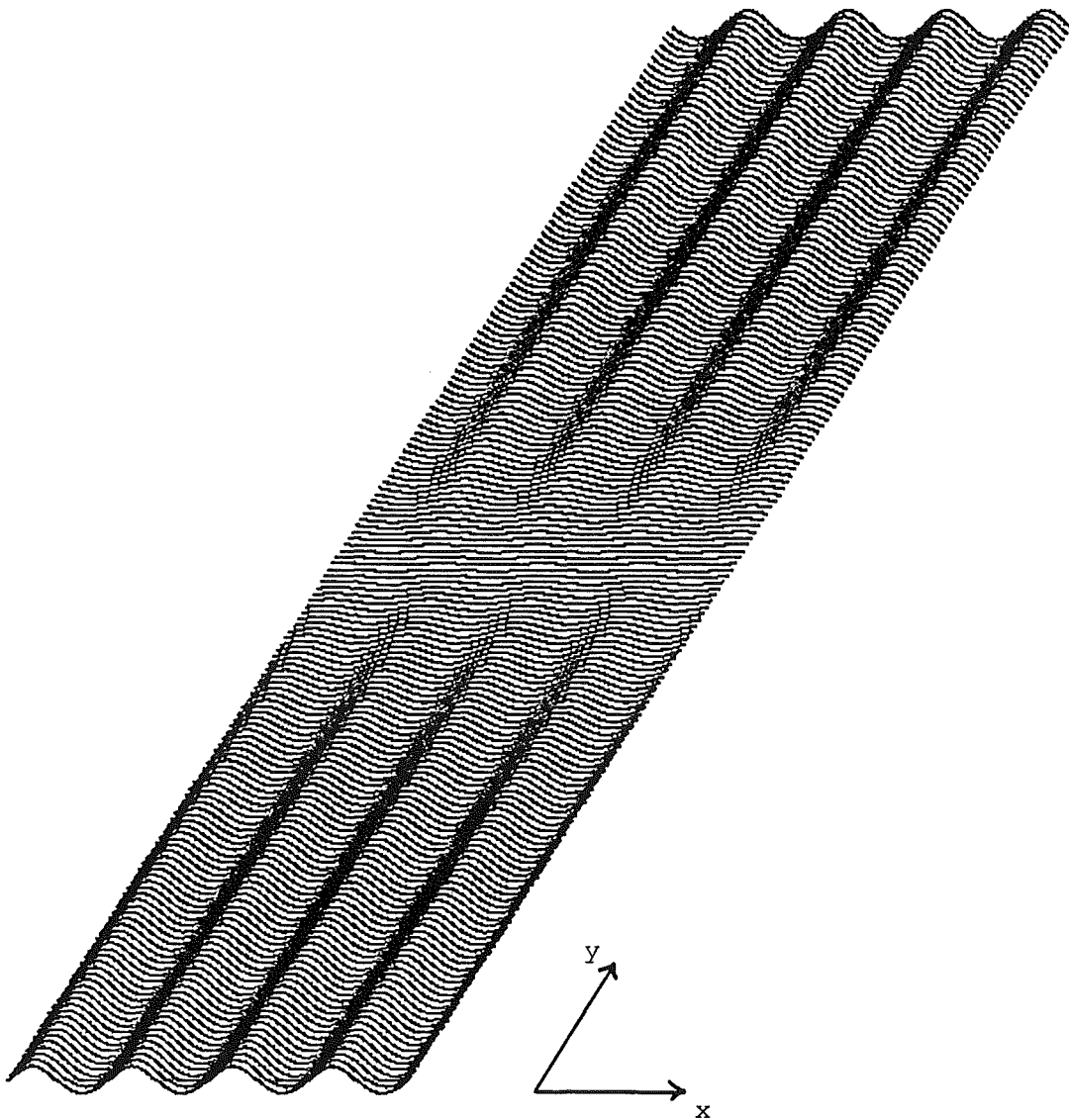


Figure 5 Perspective view of doubly-periodic waves with  $\epsilon = 0.1$ ,  $r = 100$ , showing 4 wavelengths in the x-direction and one eighth of a wavelength in the y-direction. Vertical magnification 10.



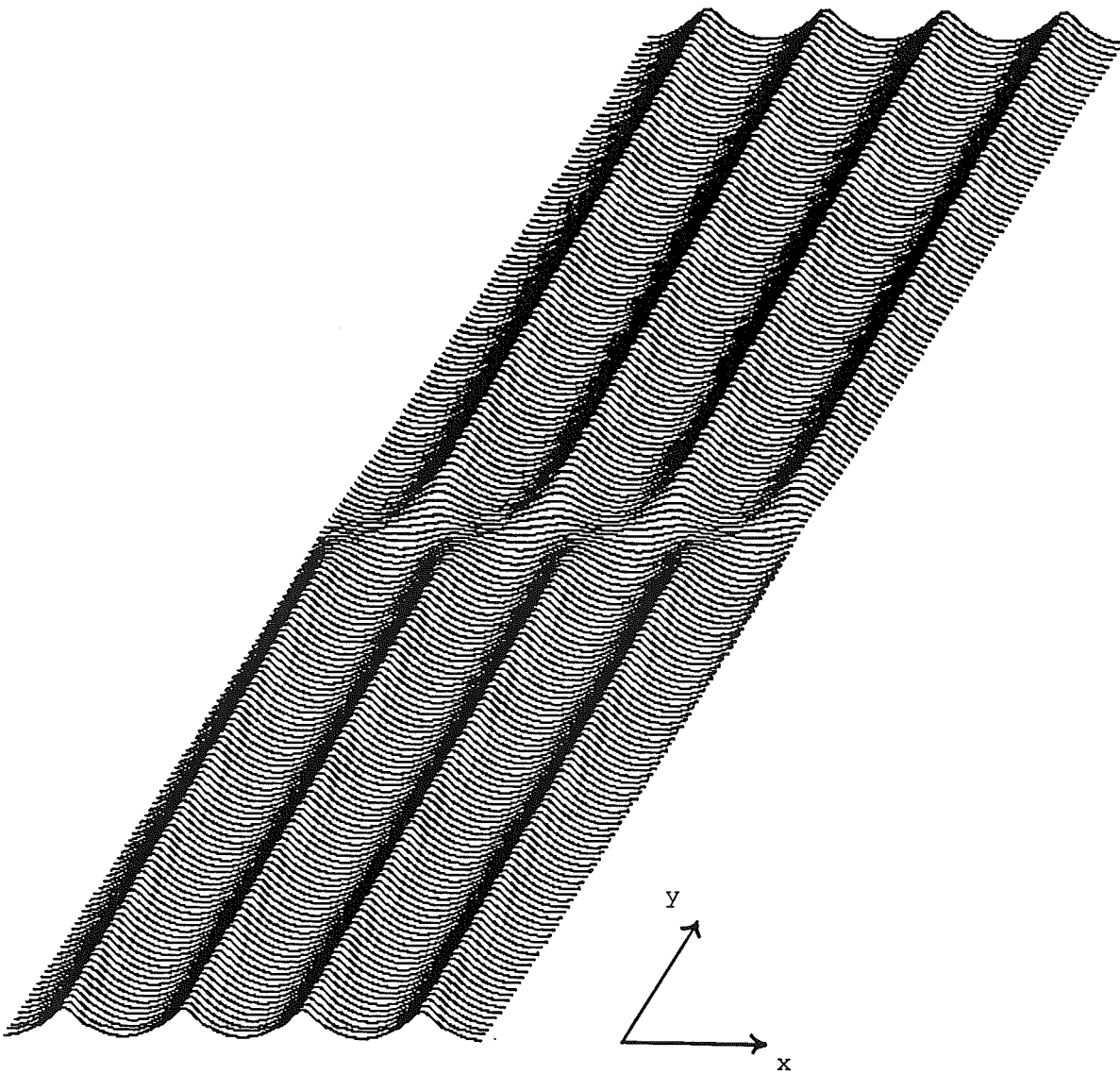


Figure 7 Perspective view of doubly-periodic waves with  $\varepsilon = 0.5$ ,  $r = 10$ , showing 4 wavelengths in the x-direction and 1 wavelength in the y-direction. Vertical magnification 2.